Phys Chem Minerals (2004) 31: 45–51
DOI 10.1007/s00269-003-0373-8

ORIGINAL PAPER

B. Lavina · G. Salviulo · A. Della Giusta

Structure modelling and cation partitioning of spinel solid solutions at high *T,P* conditions

Received: 22 May 2003 / Accepted: 21 October 2003

Abstract This paper presents evaluation of cation distributions from diffraction data collected at high *T*, *P*, and is an extension of the spinel structure modelling procedure by Lavina et al. (2002). Optimised cation-to-oxygen distances are modified for thermal expansion and compressibility at *T* and *P* of interest following Hazen and Prewitt (1977) and Hazen and Yang (1999). The procedure is applied to literature data concerning hercynite, spinel *s.s.*, Zn aluminate, Zn ferrite, magnetite and the $(Fe_3O_4)_{1-x}(MgAl_2O_4)_x$ join. Calculated cation distribution is strongly affected by standard deviations in cell parameters and oxygen coordinates. The underestimated values often reported in the literature for powder profile refinements may strongly affect the cation distribution; however, if standard deviations are increased to physically realistic values, consistent results are obtained. For *P* up to 10 GPa, reasonable evaluations of cation distribution are obtained for spinel *s.s.*, Zn aluminate and magnetite, whereas for Zn ferrite they are limited to 1.8 GPa. For *P* beyond 10 GPa, compressibility cannot be assumed to be linear; the relationship between cell parameter and pressure is well-defined, but the inaccuracy of oxygen coordinate prevents simple modelling of bond distances with pressure.

Keywords Spinel · Cation distribution · Thermal expansion · Compressibility

Introduction

The structural response of spinels in high-temperature and -pressure conditions is very important in the geosciences because their structure is one of the few models for minerals that are stable at mantle conditions. For this reason, the behaviour of this structure versus *T* and *P* has motivated several investigations (Fei et al. 1999; Harrison et al. 1999; Redfern et al. 1999; Andreozzi et al. 2000; Pavese et al. 2000; Levy et al. 2001 and references reported therein). Prediction of equation-of-state (EOS) can be satisfactorily performed (Pavese 2002) due to the geometric simplicity of this structure, from knowledge of cation-to-oxygen bond distances and their compressibility and thermal expansivities. A complication in the evaluation of EOS parameters arises from the effects of order–disorder reactions—mainly triggered by temperature—involving several cations that may be distributed over both the tetrahedral and octahedral sites of the structure. Cation ordering appreciably affects elasticity (Liebermann et al. 1977), compressibility and thermal expansion (Hazen and Yang 1999).

The present study is an extension to high *T*, *P* conditions of the site assignment procedure based on Shannon's crystal radii, recently improved by Lavina et al. (2002). The procedure (hereafter SIDR) rests on a modified set of cation-to-oxygen distances optimised using a database of 295 samples, and allows determination of the site occupancies that best satisfy chemical and structural parameters. The cation distribution is controlled by four parameters: cell edge (*a*), oxygen fractional coordinate (*u*), site scattering power (m.a.n.$_T$, m.a.n.$_M$ or b_T, b_M), and their standard deviations (σ). High-temperature data are not numerous, and most of them concern powder-diffraction experiments, where profile refinement methods usually lead to underestimation of $\sigma(a)$ and $\sigma(u)$. Therefore, cation distribution is controlled mainly by *a* and *u*, masking information carried by the scattering power of the sites.

B. Lavina (✉) · G. Salviulo · A. Della Giusta
Dipartimento di Mineralogia e Petrologia,
Università di Padova, C.so Garibaldi 37,
I-35137 Padova, Italy
e-mail: barbara@dmp.unipd.it

Adjustment of formulation for temperature and pressure

Briefly, SIDR uses a least-squares minimisation of the following function:

$$F(X_i) = \frac{1}{n}\sum_{1}^{n} {}_j\left(\frac{O_j - C_j(X_i)}{\sigma_j}\right)^2, \quad (1)$$

where X_i are the site atomic fractions of the i^{th} cation, and O_j are observed quantities, with their standard deviations σ_j. They are the four observed crystallographic parameters, i.e. cell parameter a, oxygen coordinate u, and m.a.n.$_T$, m.a.n.$_M$ or b_T, b_M, plus the chemical atomic proportions for a total of n. $C_j(X_i)$ are the corresponding quantities calculated as a function of variable cation fractions X_i. An empirical value of $\sigma = 0.0001$ was assigned to these three crystal-chemical constraints: occupancies of T and M sites and formal valence. When not reported, a value of $\sigma = 0.5\%$ was assigned to chemical proportions.

Calculated a and u were obtained from the exact relations existing between these two parameters and T–O and M–O. These, in turn, were calculated under ambient conditions as:

$$\text{T–O} = \Sigma_i^{\text{IV}} X_i^{\text{IV}} D_i + k_1^{\text{VI}} X_{\text{Fe3+}} + k_2^{\text{VI}} X_{\text{Ni2+}} \quad (2)$$

$$\text{M–O} = \Sigma_i^{\text{I}} X_i^{\text{VI}} D_i, \quad (3)$$

where ${}^{\text{IV}}D_i$ and ${}^{\text{VI}}D_i$ are the cation-to-oxygen bond distances of each cation in T and M sites. Constants k_1 and k_2 account for the influence of octahedral Fe^{3+} and Ni^{2+} on the tetrahedral bond distance through variation of the octahedral angle (Lavina et al. 2002).

To account for thermal expansion and compressibility at the T and P of interest, bond lengths D in Eqs. (2) and (3) were modified as follows:

$$D(T,P) = Do + \Delta T * \partial D/\partial T - \Delta P * \partial D/\partial P, \quad (4)$$

where D_o is the bond distance under standard conditions (23 °C, 0.0001 GPa).

As is well known, Eq. (4) is only a first-order approximation, used because of the scarcity of data on the actual dependence of bond lengths on pressure and temperature.

Values of the derivatives of bond lengths in Eq. (4) (taken from Hazen and Yang 1999) in both tetrahedral and octahedral coordination are presumed to be constant for any specific cation-to–oxygen bond up to 1000 °C and 10 GPa. Mean coefficients of bond expansion α and compression β of cations not reported by these authors were calculated with the empirical equations of Hazen and Prewitt (1977):

$$\alpha = 32.9(0.75 - z/p)10^{-6}\,^{\circ}\text{C}^{-1} \quad (5)$$

$$\beta = 37.0(D_0^3/z)10^{-5}\ \text{Gpa}^{-1}, \quad (6)$$

where z is the cation charge and p is the coordination number. Within the accuracy of the available experimental data this is fully acceptable because the derivatives of the bond lengths with respect to temperature are very similar for cations with the same valence, as also reported by Hazen and Yang (1999). To fit their α values, coefficient 0.75 in Eq. (5) was modified to 0.78 to avoid $\alpha = 0$ for trivalent cations in the T site.

Foley et al. (2001) proposed an alternative approach based on the OccQP procedure by Wright et al. (2000). Their constrained linear least-squares formulation contains bond-valence coefficients adjusted for temperature according to Brown et al. (1997). OccQp formulation is very valuable for topochemically complex structures, but for spinels, cation distributions obtained with OccQP differ substantially from those obtained using refined cation-to-oxygen bond lengths with the SIDR procedure, as discussed by Lavina et al. (2002).

As Foley et al. (2001) stress, the best test of the reliability of a cation site assignment is the final agreement between observed and modelled parameters. Consequently, any acceptable cation assignment must reproduce these parameters, possibly within their standard deviation. Results according to SIDR, like any minimisation based on χ^2, depend strongly on the σ values of any single parameter; consequently, those with underestimated σ excessively constrain cation distribution, masking information from the other parameters and leading to scattered values of residuals in Eq. 1.

Testing the modified formulation

High temperature

$FeAl_2O_4$ and $MgAl_2O_4$

In-situ neutron structural refinements were used to determine the temperature dependence of the cation distribution in synthetic hercynite and spinel *s.s.* by Harrison et al. (1998) and Redfern et al. (1999), respectively. Concerning hercynite, for all runs up to 1423 K, $F(X_i)$ values close to 1 were obtained, meaning that, on average, calculated and observed values match within one standard deviation. Nevertheless, the distribution of residuals was uneven, those relative to the site-scattering length being up to four times their σ, as a consequence of the very small $\sigma(a)$ and $\sigma(u)$ (0.00003 Å and 0.000003 as means, respectively). Because the actual σ obtained with the Rietveld refinement are estimated to be at least twice as large as in single-crystal studies (Young 1995), cation distributions were recalculated with $\sigma(a) = 0.0001$ Å and $\sigma(u) = 0.0003$, obtaining small, comparable values of residuals for all structural parameters.

Optimised inversions obtained with these two calculations are shown in Fig. 1, compared with those calculated by Harrison et al. (1998) only from site-scattering lengths. Inversions calculated with modified σ overlap experimental ones throughout the temperature range. In any case, even using these authors' standard deviations, differences were relatively small, with a maximum of about 0.02 at the lowest temperature.

Using $MgAl_2O_4$, Redfern et al. (1999) performed two sets of thermal runs up to 1600 °C at two different laboratories (RAL, UK; ANL, USA), obtaining relatively wide scattering of inversions (Fig. 2). Values optimised by SIDR were higher than experimental ones, with maximum inversion differences of up to 0.06 at the

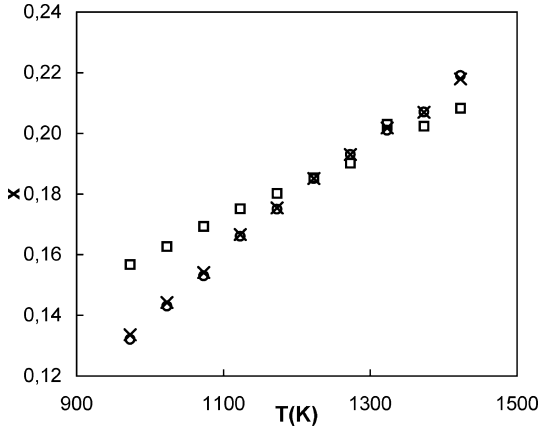

Fig. 1 Inversion (x) vs. temperature for synthetic hercynite by Harrison et al. (1998). *Crosses* Experimental data; *squares and circles* calculated data with experimental and increased σ, respectively

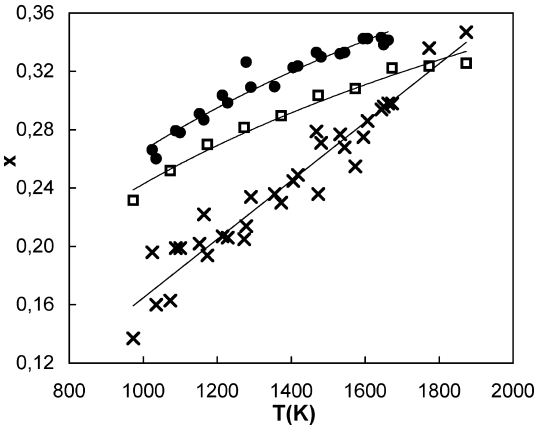

Fig. 2 Inversion (x) vs. temperature for synthetic spinel *s.s.* by Redfern et al. (1999). *Crosses* Experimental data; *squares and circles* SIDR results from RAL and ANL experimental data, respectively (see text)

lowest T. The calculated trend was also appreciably different, the increase being definitely more limited. Moreover, data from RAL were systematically lower than those from ANL, due to small but systematic differences in the oxygen fractional coordinate obtained from the data measured in the two laboratories.

As for hercynite, calculations were repeated with $\sigma(a) = 0.0001$ Å and $\sigma(u) = 0.0003$. The inversion of both sets underwent general decrease, but not sufficient to overlap the cation distribution of Redfern et al. (1999).

In $MgAl_2O_4$, unlike $FeAl_2O_4$, the inversions calculated by SIDR were substantially different from those obtained only from neutron-scattering lengths. This was not surprising because the literature data show large discrepancies in the inversion of $MgAl_2O_4$, as discussed, for example, in Andreozzi et al. (2000).

$(Fe_3O_4)_{1-x}(MgAl_2O_4)_x$

Harrison et al. (1999) investigated this solid solution at $x = 0.4$, 0.5 and 0.75 up to 1273 K by combining structural refinements—from in-situ time-of-flight neutron powder diffraction—with measurements of saturation magnetisation in quenched samples.

Table 1 compares SIDR results at low and high T with the scheme of cation distribution proposed by the above authors. Single atomic fractions show some differences, mainly at $x = 0.5$, but the authors' distribution scheme is confirmed.

Determination of four atomic fractions per site is a complex problem because the minimisation function may have several local minima. The distributions shown in Table 1 correspond to the absolute minimum of $F(X_i)$ which, under these conditions, may show non-parabolic behaviour with respect to cation distribution. Moreover, from the simultaneous presence of both Fe^{2+} and Fe^{3+}, electron hopping in M site may also be possible in the iron-richer composition, but attempts to introduce octahedral $Fe^{2.5+}$ led to drastic worsening of $F(X_i)$.

Harrison et al. (1999) also performed annealing runs for $x = 0.75$ at $T = 923$ K, increasing times up to 3960 s. Their results revealed a two-stage process: in stage 1, up to 1400 s, a increased sharply, but very slowly in stage 2. These authors state that their derived cation distributions—which require ordering of Fe^{3+} in T site—contrasted with thermodynamic models (O'Neill and Navrotsky 1984; Nell et al. 1989). Using SIDR, unacceptable $F(X_i)$ values were obtained (minimisation 1), mainly due to disagreement in scattering lengths ($\Delta b_T = 0.2$–0.4, $\Delta b_M = 0.1$–0.2). As in the former example, minimisation was repeated with $\sigma(a) = 0.0001$ and $\sigma(u) = 0.0003$ (minimisation 2). Better fits of b_T and b_M were obtained, and $F(X_i)$ decreased to values close to 2, with similar values for all residuals. Figure 3 shows that both minimisations led to cell edges consistent with those of Harrison et al. (1999), whereas the trend of u was reproduced only by minimisation 1, but with slightly higher values. The more reliable minimisation 2 gave u values definitely higher than the experimental ones, and a definite slope with an increase from 0.2613 to 0.2619. The corresponding cation distributions reported in Table 2 suggest ordering of large divalent cations in the T site and small trivalent cations in the M site. It is emphasised that this ordering is in agreement with the quoted thermodynamic models.

High pressure

High-pressure data are sometimes affected by quite large aberrations and uncertainties. Recent experiments by Pavese et al. (1999) and Levy et al. (2000, 2001) on synthetic $MgAl_2O_4$, $ZnAl_2O_4$ and $ZnFe_2O_4$ confirmed that, up to about 10 GPa, pressure derivatives may be

Table 1 $(Fe_3O_4)_{1-x}(MgAl_2O_4)_x$ Observed and calculated tetrahedral cations distribution for three different compositions at two temperatures

	x = 0.4				x = 0.5				x = 0.75			
T (K)	873		1273		873		1273		938		1273	
$F(X_i)$		19		2.0		1.4		2.3		5.3		13
	obs	calc	obs	calc	obs	calc	obs	calc	obs	calc	obs	calc
Fe^{3+}	0.54	0.51	0.45	0.44	0.43	0.39	0.42	0.36	0.28	0.22	0.18	0.19
Fe^{2+}	0.26	0.28	0.30	0.32	0.25	0.26	0.24	0.27	0.16	0.14	0.16	0.15
Mg	0.18	0.20	0.21	0.22	0.25	0.30	0.24	0.33	0.48	0.53	0.54	0.53
Al	0.02	0.01	0.04	0.02	0.07	0.05	0.10	0.04	0.08	0.11	0.12	0.12

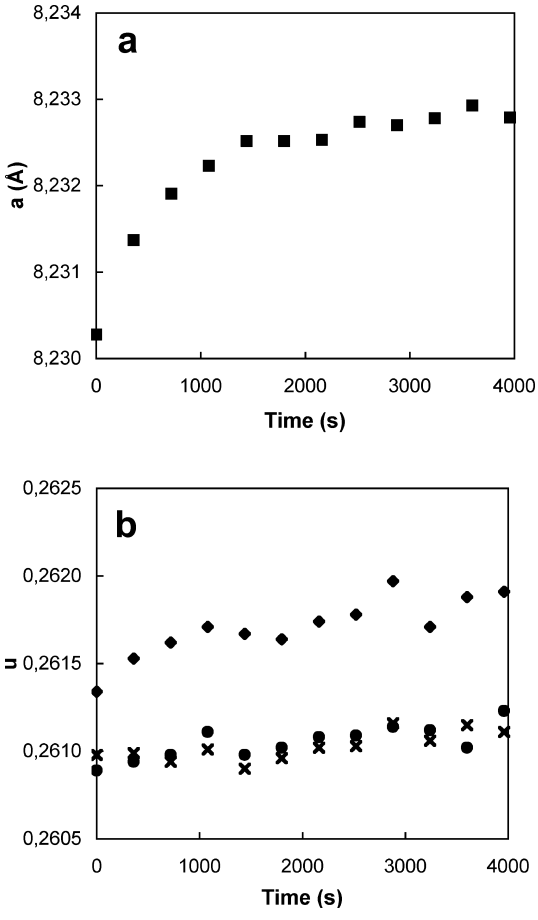

Fig. 3a, b Structural parameters vs. annealing time of synthetic $(Fe_3O_4)_{0.25}(MgAl_2O_4)_{0.75}$ by Harrison et al. (1999). *Crosses* Experimental data; *circles and diamonds* calculated data with experimental and increased σ. **a** Cell edge: all data overlap. **b** Oxygen fractional coordinate

reasonably assumed to be constant. Beyond these values, compressibility showed the well-known progressive decrease, clearly evidenced by the trend of cell parameter versus pressure (Fig. 4a) that, for the quoted experiments, may be very accurately described ($R^2 > 0.99$) as:

$$a_P = a_0 - c_1P + c_2P^2, \quad (7)$$

where a_0 and a_P are cell parameters at ambient pressure and at the P of interest, and c_1 and c_2 are fitting constants specific for each composition. Unfortunately, the trend of bond distances versus P cannot be described with the same accuracy. Figure 4b shows that Zn ferrite had completely different behaviour and that its data were more scattered than those of other samples. This prevented modification of Eq. (6) in order to estimate β variations in bond lengths as a function of pressure; consequently, only data up to 10 GPa are discussed here. Experimental complications in high-P diffraction experiments sometimes do not allow reliable evaluation of scattering lengths or mean atomic numbers of individual sites, so that structure modelling must rely mainly on geometric parameters.

$MgAl_2O_4$

Finger et al. (1986) and Pavese et al. (1999) investigated a natural gem-quality crystal ($Mg_{1.020}$ $Al_{1.970}$ $Fe^{3+}_{0.007}$ $Zn_{0.006}$ O_4) up to 4 GPa, and a synthetic Mg–Al spinel containing about 0.02 vacancies ($Mg_{0.95}$ $Al_{2.030}$ $Vac_{0.020}$ O_4) up to 29 GPa. Results of SIDR are shown in Table 3a and b.

Using the data of Finger et al. (1986), minimisation of $F(X_i)$ was performed with minor elements, Fe and Zn, fixed in M and T, respectively. Structure parameters were all reproduced within 1σ. Only the squared residual (Eq. 1) for bulk chemistry was relatively larger, up to 5σ. This pointed to the relative inconsistency of the chemical analysis, which reported an excess of Mg, rather uncommon in natural Mg–Al spinel, whereas the mean bulk chemistry calculated by SIDR was $Mg_{0.994}$ $Al_{1.993}$ $Fe^{3+}_{0.007}$ $Zn_{0.006}$ O_4. In spite of the very limited number of reflections collected (about 45), the calculated cation distribution is reasonable; the calculated inversion Al(T) in Table 3a shows a relatively narrow spread, with a mean value of 0.16(2), with no systematic trend with pressure.

Table 2 $(Fe_3O_4)_{0.25}(MgAl_2O_4)_{0.75}$ calculated parameters for different annealing times. $\Sigma M^{3+}{}_T$, $\Sigma M^{2+}{}_T$: sum of trivalent and bivalent cations in the T site. Time in s

Time	F(x_i)	a	u	Al_T	$Fe^{2+}{}_T$	$Fe^{3+}{}_T$	Mg_T	$\Sigma M^{3+}{}_T$	$\Sigma M^{2+}{}_T$
Stage 1									
0	0.8	8.2303	0.26134	0.096	0.124	0.219	0.561	0.315	0.685
360	1.0	8.2313	0.26153	0.089	0.128	0.206	0.577	0.295	0.705
720	1.9	8.2319	0.26162	0.081	0.134	0.211	0.574	0.292	0.708
1080	1.8	8.2322	0.26171	0.074	0.131	0.209	0.585	0.283	0.716
1440	2.4	8.2325	0.26167	0.061	0.114	0.233	0.592	0.294	0.706
1800	2.3	8.2325	0.26164	0.079	0.132	0.211	0.578	0.290	0.710
Stage 2									
2160	1.8	8.2325	0.26174	0.074	0.132	0.207	0.587	0.281	0.719
2520	2.0	8.2327	0.26178	0.076	0.137	0.198	0.589	0.274	0.726
2880	1.8	8.2327	0.26197	0.062	0.142	0.201	0.595	0.263	0.737
3240	1.5	8.2328	0.26171	0.081	0.130	0.195	0.594	0.276	0.724
3600	1.9	8.2329	0.26188	0.073	0.144	0.193	0.590	0.266	0.734
3960	2.0	8.2328	0.26191	0.074	0.151	0.190	0.585	0.264	0.736

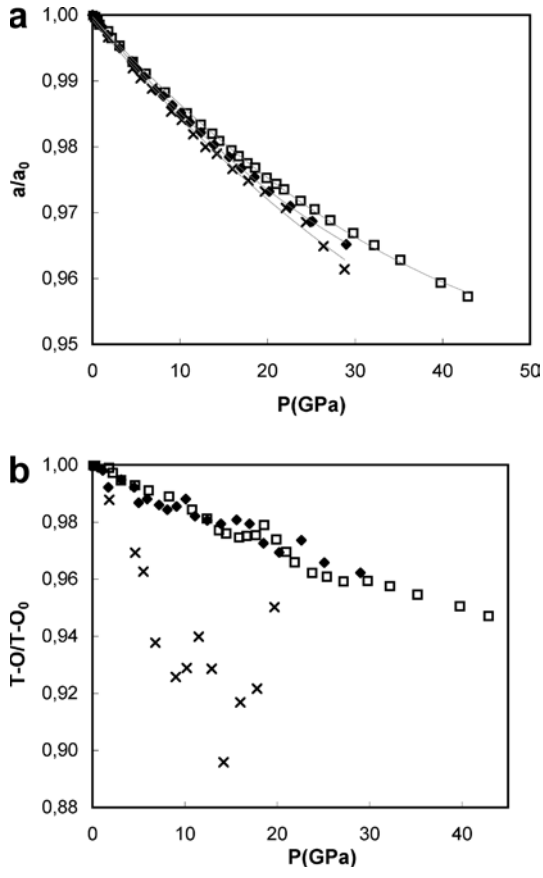

Fig. 4a, b Compressibility of **a** cell edge and **b** tetrahedral bond distance versus pressure. *Diamonds* Mg aluminate; *squares* Zn aluminate; *crosses* Zn ferrite. *Solid lines* in **a** are polynomial fits of experimental data, for each one, R^2 is greater than 0.995

Data by Pavese et al. (1999), up to 5.0 GPa, show the good fit of both structural and chemical parameters, with very low F(X_i) values. In this P range, the amount of Al(T) remained almost unchanged with increasing pressure, with a mean value of 0.20(2) (Table 3b), higher than that found by Finger et al. (1986), as expected from a synthetic sample with respect to a natural, slowly cooled one. The calculated inversion was also in good agreement with the value of 0.21(1) derived by Pavese et al. (1999) using different schemes of vacancy distributions, including a defect-free model. SIDR indicated the preference of vacancies for the M site, and evidenced the full consistency of the experimental data, including bulk chemistry. Above 5.0 GPa, drastic worsening of F(X_i) began, due to attempts by the minimisation process to increase the Mg/Al ratio as a way of compensating for the decrease in compressibility.

$ZnAl_2O_4$ and $ZnFe_2O_4$

High-pressure neutron powder diffraction runs were performed on Zn aluminate ($Zn_{0.97}\ Al_{2.02}\ Vac_{0.01}\ O_4$) up to 42.9 GPa and on Zn ferrite ($Zn_{0.970}\ Fe_{2.020}\ Vac_{0.010}\ O_4$) up to 24 GPa by Levy et al. (2001) and Levy et al. (2000), respectively. The results of the minimisation procedure are listed in Table 3c and d.

Table 3 Optimisation results of high-pressure data. Δa, ΔT–O, ΔM–O: differences between observed and calculated data, M^{3+}(T): tetrahedral trivalent cations. **a** Spinel *s.s*; **b** Mg aluminate; **c** Zn aluminate; **d** Zn ferrite; **e** magnetite (Nakagiri et al. 1986); **f** magnetite (Finger et al. 1986)

	P(Gpa)	F(X_i)	$\Delta a/\sigma$	ΔT−O/σ	ΔM−O/σ	M^{3+}(T)
a	0.0001	4.4	−0.7	1.0	−0.5	0.16
	1.00	4.3	−0.2	0.3	−0.2	0.14
	2.00	4.3	0.3	−0.2	0.2	0.18
	3.00	4.3	0.2	−0.4	0.3	0.13
	4.00	4.6	−1.0	1.5	−1.0	0.19
b	0.0001	1.7	0.0	0.2	0.0	0.21
	1.1	1.3	0.0	−0.5	0.0	0.20
	3.1	1.9	0.0	−0.7	0.3	0.19
	5.0	2.4	0.2	−4	2	0.20
	7.2	3.9	0.6	−5	3	0.14
	8.1	15	1	−10	5	0.12
c	0.0001	19	0.6	10	−6	0.05
	0.8	12	1	10	−6	0.04
	1.8	18	1.1	10	−5	0.05
	2.2	8.2	0.9	9	−5	0.04
	3.1	7.3	1	0.8	−3	0.04
	4.6	2.8	0.2	7	−4	0.03
	6.1	4.9	0.2	9	−5	0.04
	8.3	7.6	0.3	10	−5	0.05
	10.8	8.6	0.8	0.6	−3	0.02
d	0.0001	6.9	2	2	−1	0.03
	1.8	1.6	−0.3	−6	3	0.03
	4.6	20	−1.5	−14	8	0.11
	5.5	29	−1.9	−15	8	0.06
	6.8	21	−1	−20	11	0.37
	9.0	14	0.2	−13	7	0.78
	10.2	46	−1.6	−32	18	0.07
e	0.0001	0.4	0.8	1.1	−0.8	1.00
	0.63	1.9	1.5	−2.5	1.5	1.00
	1.55	1.2	0.8	−1.8	1.0	1.00
	2.09	0.6	0.5	−2.0	1.1	1.00
	2.76	0.3	0.5	0.01	−0.1	1.00
	3.67	3.0	0.7	−2.7	1.6	1.00
	4.4	0.8	0.4	−1.2	0.9	1.00
f	0.0001	0.3	0.2	2.9	−2.0	1.00
	1.3	0.3	−1.0	2.0	−1.5	1.00
	2.6	0.3	−1.2	0.2	−0.2	1.00
	3.9	0.8	−1.5	1.2	−1.0	1.00
	4.5	0.3	1.0	1.5	−0.9	1.00

High F(X_i) in Zn aluminate (Table 3c) were due to the systematic bad fit of bond distances, already shown at ambient pressure: experimental parameters were a = 8.09117(5)Å, u = 0.2654(2), and consequently T–O was 1.976 Å, definitely larger than 1.960 Å, the Zn–O bond distance used by SIDR. These parameters were even greater than those of the non-defect Zn aluminate by O'Neill and Dollase (1994) [a = 8.0869(1)Å, u = 0.2643(3)], whereas they should be smaller, due to the excess of trivalent cation as in Mg–Al compositions (Lucchesi and Della Giusta 1994). The calculated

inversion of about 0.04 is consistent with the results reported by Levy et al. (2001), and remains unchanged with increasing P.

In Zn ferrite, the a and u values reported by Levy et al. (2000) [$a = 8.4412(2)$Å, $u = 0.2605(2)$] at ambient P were not consistent with their bulk chemistry ($Zn_{0.97}\ Fe^{2+}_{2.02}\ Vac_{0.01}\ O_4$) but in good agreement with those reported by O'Neill (1992) [$a = 8.4419(2)$Å, $u = 0.2604(2)$] for a non-defect sample. The agreement between observed and calculated a and u was satisfactory only up to 1.8 GPa, after which $F(X_i)$ worsened drastically (Table 3d). The decrease in T–O, which was about twice that of Zn aluminate, could not be fitted using Eq. (6), and may be explained by a strong increase in inversion, but this hypothesis contrasts with the tetrahedral preference of Zn, at least under ambient conditions.

The failure of SIDR may also be explained by considering the k_1 coefficient in the formulation of T–O bond length (Eq. 2). This coefficient accounts for T–O changes caused at ambient P by modifications in the octahedral angle in the presence of $^{VI}Fe^{3+}$, but its behaviour with pressure is unknown. Consequently, β values for T–O and M–O are at least partly correlated, an effect currently difficult to deal with in non-ambient conditions.

Fe_3O_4

Magnetite was investigated up to 4.5 GPa by Nakagiri et al. (1986) and Finger et al. (1986). Table 3e and f shows that, in both cases, results are consistent, almost all parameters fitting within 2σ. Fe^{2+} and Fe^{3+} were variable parameters in both T and M sites, and, in M, equal amounts of the two species were allowed to form $Fe^{2.5+}$ via electron hopping (Marshall and Dollase 1984). Calculated bulk chemistry was fully consistent with structural parameters, as shown by the $F(X_i)$ values, always less than 3, and less than 1 for runs by Finger et al. (1986). Consequently, the amounts of calculated $^{IV}Fe^{3+}$, always very close to 1, suggest that, in the investigated range of pressure, no change of inversion occurs, unlike the effects of temperature evidenced by Wu and Mason (1981).

Concluding remarks

The self-consistency of spinel diffraction data, at both high temperature and pressure, was tested with the SIDR procedure, modifying cation-to-oxygen bond lengths for thermal expansion and compressibility with the approach of Hazen and Prewitt (1977) and Hazen and Yang (1999).

The uncertainties in expansivity and compressibility coefficients affect the cations partitioning to an amount that can be roughly estimated assuming an uncertainty of 5% for $\partial D/\partial T$ and 15% for $\partial D/\partial P$, respectively, in the data by Hazen and Yang (1999). Distributions recalculated with expansivity of the involved cations modified by 5% led to changes of the site atomic fractions up to 0.02 afu, while changes up to 0.04 afu were obtained with the assumed uncertainty of compressibility. This result is rather satisfactory, since a realistic uncertainty of atomic fractions obtained with SIDR from data at ambient conditions is 0.01 afu as a mean (Lavina et al. 2002).

Results were highly reliable when structural data and scattering lengths or mean atomic numbers were accurately measured. The SIDR results, as in any procedure based on chi-squared, were very sensitive to the standard deviations of the experimental parameters. Most of the examined data are from profile powder refinements, which underestimate the standard deviations of the refined parameters. In these cases, SIDR leads to uneven distribution of minimised residuals, with bad fitting of chemical composition. Satisfactory agreement of all modelled parameters was reached when the sigma values obtained in single-crystal experiments were used. With these assumptions, even with several cations in each site, cation distributions consistent with thermodynamic models can be predicted.

For high P runs, variations in a and bond distances beyond 10 GPa cannot be defined with the same accuracy due to the poorer quality of the experimental data. This is a consequence of experimental problems in intensity evaluation, which mainly affect the determination of u, as revealed in some cases by discrepancies in data measured at ambient conditions. Problems related to the decrease in compressibility become crucial above about 10 GPa. Beyond this value, presently available data do not allow Eq. (6) to be modified in a reliable way. Below this value, reasonable evaluations of the cation distribution are in any case obtained for $MgAl_2O_4$, $ZnAl_2O_4$ and magnetite.

Acknowledgements Contributions by referees J.M.Hughes and A. Pavese are gratefully acknowledged. This work was financially supported by an MURST grant (A. Della Giusta, COFIN 2001: Intracrystalline ordering-disordering processes in rock-forming minerals). Thanks are due to Ms. Gabriel Walton, who revised the English text.

References

Andreozzi GB, Princivalle F, Skogby H, Della Giusta A (2000) Cation ordering and structural variations with temperature in $MgAl_2O_4$ spinel: an X-ray single-crystal study. Am Mineral 85: 1164–1171

Brown I, Dabkowski A, McCleary A (1997) Thermal expansion of chemical bonds. Acta Crystallogr (B) Struct Sci 53: 750–761

Fei Y, Frost DJ, Mao HK, Prewitt CT, Häusermann D (1999) In situ structure determination of the high–pressure phase of Fe_3O_4. Am Mineral 84: 203–206

Finger LW, Hazen RM, Hofmeister AM (1986) High-pressure crystal chemistry of spinel ($MgAl_2O_4$) and magnetite (Fe_3O_4): comparison with silicate spinels. Phys Chem Miner 13: 215–220

Foley JA, Wright SE, Hughes JM (2001) Cation partitioning versus temperature in spinels: optimization of site occupants. Phys Chem Miner 28: 143–149

Harrison RJ, Dove MT, Knight KS, Putnis A (1999) In-situ neutron diffraction study of non-convergent cation ordering in the $(Fe_3O_4)_{1-x}(MgAl_2)O_4$ spinel solid solution. Am Mineral 84: 555–563

Harrison RJ, Redfern SAT, O'Neill HSC (1998) The temperature dependence of the cation distribution in synthetic hercynite ($FeAl_2O_4$) from in-situ neutron structure refinements. Am Mineral 83: 1092–1099

Hazen RM, Prewitt CT (1977) Effects of temperature and pressure on interatomic distances in oxygen-based minerals. Am Mineral 62: 309–315

Hazen RM, Yang H (1999) Effects of cation substitution and order-disorder on *P–V–T* equations of state of cubic spinels. Am Mineral 84: 1956–1960

Lavina B, Salviulo G, Della Giusta A (2002) Cation distribution and structure modelling of spinel solid solutions. Phys Chem Miner 29: 10–18

Levy D, Pavese A, Hanfland M (2000) Phase transition of synthetic zinc ferrite spinel ($ZnFe_2O_4$) at high pressure, from synchrotron X-ray powder diffraction. Phys Chem Miner 27: 638–644

Levy D, Pavese A, Sani A, Pischedda V (2001) Structure and compressibility of synthetic $ZnAl_2O_4$ (gahnite) under high-pressure conditions, from synchrotron X-ray powder diffraction. Phys Chem Miner 28: 612–618

Liebermann R, Jackson I, Ringwood A (1977) Elasticity and phase equilibria of spinel disproportionation reactions. Geophys J Roy Astron Soc 50: 553–586

Lucchesi S, Della Giusta A (1994) Crystal chemistry of non-stoichiometric Mg–Al synthetic spinels. Z Kristallogr 209: 714–719

Marshall CP, Dollase WA (1984) Cation arrangement in iron-zinc-chromium spinel oxides. Am Mineral 69: 928–936

Nakagiri N, Manghnani M, Ming L, Kimura S (1986) Crystal structure of magnetite under pressure. Phys Chem Miner 13: 238–244

Nell J, Wood B, Mason T (1989) High-temperature cation distribution in Fe_3O_4–$MgAl_2O_4$–$MgFe_2O_4$–$FeAl_2O_4$ spinels from thermopower and conductivity measurements. Am Mineral 74: 339–351

O'Neill HSC (1992) Temperature dependence of the cation distribution in zinc ferrite ($ZnFe_2O_4$) from powder XRD structural refinements. Eur J Mineral 4: 571–580

O'Neill HSC, Dollase WA (1994) Crystal structures and cation distributions in simple spinels from powder XRD structural refinements: $MgCr_2O_4$, $ZnCr_2O_4$, Fe_3O_4 and the temperature dependence of the cation distribution in $ZnAl_2O_4$. Phys Chem Miner 20: 541–555

O'Neill HSC, Navrotsky A (1984) Cation distribution and thermodynamic properties of binary spinel solid solutions. Am Mineral 69: 733–753

Pavese A (2002) Pressure-volume-temperature equations of state: a comparative study based on numerical simulations. Phys Chem Miner 29: 43–51

Pavese A, Artioli G, Hull S (1999) Cation partitioning versus pressure in $Mg_{0.94}Al_{2.04}O_4$ synthetic spinel, by in situ powder neutron diffraction. Am Mineral 84: 905–912

Pavese A, Levy D, Hoser A (2000) Cation distribution in synthetic zinc ferrite ($Zn_{0.97}$ $Fe_{2.02}O_4$) from in situ high-temperature neutron powder diffraction. Am Mineral 85: 1497–1502

Redfern SAT, Harrison RJ, O'Neill HSC, Wood DRR (1999) Thermodynamics and kinetics of cation ordering in $MgAl_2O_4$ spinel up to 1600 °C from in situ neutron diffraction. Am Mineral 84: 299–310

Wright SE, Foley JA, Hughes JM (2000) Optimisation of site occupancies in minerals using quadratic programming. Am Mineral 85: 524–531

Wu C, Mason T (1981) Thermopower measurement of cation distribution in magnetite. J Am Ceram Soc 64: 520–522

Young RA (1995) The Rietveld method. Oxford Science Publications, Oxford, pp 298